Chymase Inhibition Reduces the Progression to Heart Failure After Autoimmune Myocarditis in Rats

Suresh S. Palaniyandi,*,†,[1] Yusuke Nagai,*,[1] Kenichi Watanabe,*,[2] Meilei Ma,* Punniyakoti T. Veeraveedu,* Paras Prakash,* Fadia A. Kamal,* Yuichi Abe,* Ken'ichi Yamaguchi,‡ Hitoshi Tachikawa,§ Makoto Kodama,§ and Yoshifusa Aizawa§

*Department of Clinical Pharmacology, Niigata University of Pharmacy and Applied Life Sciences, Niigata City, 956-8603, Japan; †Department of Chemical and Systems Biology, Stanford University School of Medicine, Stanford, CA 94305; ‡Department of Homeostatic Regulation and Development, Niigata University School of Medicine, Niigata City, 951-8510, Japan; and §First Department of Medicine, Niigata University School of Medicine, Niigata City, 951-8510, Japan

Chymase has been known as a local angiotensin II–generating enzyme in the cardiovascular system in dogs, monkeys, hamsters, and humans; however, recently it was reported that chymase also has various other functions. Therefore, we decided to examine whether the inhibition of chymase improves disease conditions associated with the pathophysiology of dilated cardiomyopathy in rats and its possible mechanism of action as rat chymase is unable to produce angiotensin II. We examined the effect of TY-51469, a novel chymase inhibitor (0.1 mg/kg/day [group CYI-0.1, *n* = 15] and 1 mg/kg/day [group CYI-1, *n* = 15]), in myosin-immunized postmyocarditis rats. Another group of myosin-immunized rats was treated with vehicle (group V, *n* = 15). Age-matched normal rats without immunization (group N, *n* = 10) were also included in the study. After 4 weeks of treatment, we evaluated cardiac function; area of fibrosis; fibrogenesis; levels of transforming growth factor (TGF)-β1 and collagen III; hypertrophy and its marker, atrial natriuretic peptide (ANP); and mast cell activity. Survival rate and myocardial functions improved dose-dependently with chymase inhibitor treatment after myosin immunization. A reduction in the percent area of myocardial fibrosis, fibrogenesis, myocardial hypertrophy, and mast cell activity along with a reduction in TGF-β1, collagen III, and ANP levels in the myocardium were noted in postmyocarditis rats that received chymase inhibitor treatment. The treatment also decreased myocardial aldosterone synthase levels in those animals. Inhibition of chymase reduces the pathogenesis of postmyocarditis dilated cardiomyopathy and progression to heart failure by preventing the pathological remodeling and residual inflammation in rats. Exp Biol Med 232:1213–1221, 2007

Key words: chymase inhibitor; cardiomyopathy; postmyocarditis rats; mast cells

Introduction

Chymase is stored intracellularly in the secretary granules of mast cells and is released upon mast cell activation (1). Mast cell degranulation is expected to be stimulated in chronic inflammatory states, thus releasing a large number of inflammatory mediators, including chymase (2–4). Indeed, the infiltration and the proliferation of mast cells are induced in failing hearts (5, 6) where the number of chymase-positive mast cells is also increased (7).

Chymase mediates angiotensin (Ang) II generation primarily in hamsters, dogs, and humans (8). Ang II, in turn, stimulates hypertrophy of the myocardium and proliferation of interstitial fibroblasts and promotes cardiac remodeling in hamsters (9). Moreover, it has become clear that chymase possesses other functions such as induction of apoptosis in myocytes (10) and proliferation of noncardiomyocytes (i.e., fibrosis in neonatal rats' cell culture [10]) and stimulation of the release of collagen III and transforming growth factor (TGF)-β1 (7, 10). In an earlier study it was demonstrated that expression of the mast cell chymase gene is upregulated in the acute phase of viral myocarditis in mice, and it

This research was supported by grants from Yujin Memorial Grant; the Ministry of Education, Culture, Sports, Science and Technology of Japan; and the Promotion and Mutual Aid Corporation for Private Schools of Japan.

[1] These authors contributed equally to this work.

[2] To whom correspondence should be addressed at Department of Clinical Pharmacology, Niigata University of Pharmacy and Applied Life Sciences, Niigata City, 956-8603, Japan. E-mail: watanabe@nupals.ac.jp

Received March 19, 2007.
Accepted May 29, 2007.

DOI: 10.3181/0703-RM-85
1525-3702/07/2329-1213$15.00

remains elevated in the late phase of heart failure; thus, chymase was implicated in the myocardial necrosis, inflammation, and remodeling process of myocarditis (11). Hence, it can be conceived that chymase might play an important role in the pathophysiology of postmyocarditis dilated cardiomyopathy (DCM) in rats.

Reports that have described chymase involvement in cardiac remodeling through pathways other than Ang II mediation prompted us to investigate the mechanism of chymase-mediated cardiac remodeling in a set-up that is independent of Ang II generation by chymase. Because rat chymase is unable to mediate Ang II generation (12–14), we decided to study the effect of TY-51469, a novel benzothiophenesulfonamide derivative with potent chymase inhibitory action, in rats with DCM after autoimmune myocarditis and its possible mechanism of action.

Materials and Methods

Animals and Experimental Protocol. Nine-week-old male Lewis rats (Charles River Japan, Inc., Kanagawa, Japan) were used in the present study. Cardiac myosin prepared from the ventricular muscle of pig hearts was injected subcutaneously into the footpads of rats according to a procedure described elsewhere (15, 16). Twenty-eight days after immunization, the surviving rats were divided into three groups. Two groups of animals were treated with TY-51469, a chymase inhibitor (Toa Eiyo Ltd., Tokyo, Japan): group CYI-0.1 ($n = 15$) received 0.1 mg/kg/day, whereas group CYI-1 ($n = 15$) received 1 mg/kg/day. The third group was treated with vehicle (group V, $n = 15$). The age-matched normal control group (group N, $n = 10$) consisted of nonimmunized Lewis rats.

TY-51469 was first dissolved in 100 m*M* NaOH, then diluted with 67 m*M* phosphate buffer for each dose, and used to fill an osmotic pump (Alza Corporation, Palo Alto, CA). An indwelling cannula (PE50: Becton Dickinson and Company, Parsippany, NJ) was implanted in the right jugular vein of each rat and was connected to an osmotic pump inserted within a subcutaneous pocket. The osmotic pump was maintained to release the drug solution continuously at a rate of 2.5 μl/hr for 28 days. Throughout the experiments, all the animals were treated in accordance with our institute's guidelines for animal experimentation.

Hemodynamic and Echocardiographic Studies. To obtain hemodynamic data, rats were anesthetized with 2% halothane in oxygen during the surgical procedures. A catheter-tip transducer (Miller SPR 249; Miller Instruments, Houston, TX) was introduced into the left ventricle through the right carotid artery for the determination of peak left ventricular pressure (LVP) and left ventricular end-diastolic pressure (LVEDP), and the rates of intraventricular pressure rise (max. dP/dt) and decline (min. dP/dt) were recorded as described previously (16). After instrumentation the concentration of halothane was reduced to 0.5% to minimize the anesthetic effect on hemodynamic parameters. Echocardiographic studies were carried out with a 7.5-MHz transducer (Aloka Inc., Tokyo, Japan). The left ventricular dimensions in diastole (LVDd) and systole (LVDs) and percent fractional shortening (FS) were estimated by using the M-mode measurements.

Histopathology. The body weight (BW) of rats was noted just before anesthesia was induced. After the hemodynamic and echocardiographic analyses, the rats were sacrificed, and the myocardium was isolated and weighed to calculate the ratio of heart weight (HW) to BW. The excised myocardium was kept in formalin and the midventricle sections were then embedded with paraffin. The paraffinized midventricle sections stained with Azan-Mallory dye and a color image analyzer (CIA-102; Olympus, Tokyo, Japan) were used to quantify the area of myocardial fibrosis (blue areas were fibrotic, whereas red areas were myocardium). The results are presented as the ratio of the fibrotic area to the area of normal myocardium.

Measurement of Mean Cardiomyocyte Area. Paraffin-embedded left ventricular tissue sections stained with hematoxylin-eosin were utilized to measure cardiomyocyte area. A high-power microscope aided by a camera and computer system (BH2-RFCA; Olympus) was used. We took the advantage of View Finder and Studio Lite software applications. View Finder helps in focusing, whereas Studio Lite is useful in the selection and capture of images at higher magnifications. The magnification fields were standardized with a micrometer. Short-axis and long-axis diameters of cardiomyocytes were measured in a blinded manner by using the standardized magnification (×400). At least 10 high-power fields were selected randomly from each slide. A minimum of 100 cardiomyocytes for each group was included to calculate the mean cardiomyocyte area. The unit of mean cardiomyocyte area was μm^2.

Mast Cell Staining and Quantitation. Histochemical staining with toluidine blue was performed to identify mast cells. Briefly, slides of paraffinized midventricle sections were dewaxed, rehydrated, incubated with 0.05% (w/v) toluidine blue for 30 min, and subsequently counterstained with 0.01% (w/v) eosin for 1 min. Metachromatic staining of mast cell granules was useful in identifying these cells. Mast cell density (MCD) was quantified by counting the number of toluidine blue–positive mast cells per field (×100). At least 15 fields were included in each slide for counting.

Measurement of Histamine Concentration in Heart Tissue. Histamine was extracted from heart tissue and estimated by using a fluorometer in accordance with the procedure described elsewhere (17). The extracted histamine from the cardiac homogenate formed a complex with orthophthaldialdehyde (OPT) (Sigma, Tokyo, Japan). The fluorescence of histamine-orthophthaldialdehyde fluorophor was maximized in the presence of citric acid and measured with a spectrofluorophotometer (Shimadzu, Kyoto, Japan) at 358 nm (activation wavelength) and 446 nm (fluorescence wavelength). The concentration of cardiac histamine was expressed as μg/g of wet heart tissue.

Quantitation of Chymase Activity in Myocardium. Chymase activity was quantified by an enzymatic histochemical staining procedure adopted from a previous report (7). Formalin-fixed, paraffin-embedded midventricle sections were used for the detection of chymase activity with the help of a kit (Sigma). The slides were deparaffinized, rehydrated, and then incubated with naphthol AS-D chloroacetate in the presence of freshly formed diazonium salt and fast red violet as described in the procedure given by the manufacturer. Reddish pink coloration was regarded as a positive reaction for chymase activity. At least 100 fields were counted randomly in each slide, and the data were plotted as a graph.

Western Immunoblotting. The myocardial tissue samples obtained from different groups were homogenized with lysis buffer. Protein concentrations in these homogenized samples were measured by the bicinchoninic acid method. For Western blot analysis, proteins were separated by SDS-PAGE and identified with the following antibodies to quantify the myocardial levels of various proteins: anti–rat aldosterone synthase (AS) (Chemicon International, Temecula, CA) and anti–cyclin D1 (Cell Signaling Technology, Beverly, MA) mouse monoclonal antibodies; anti–atrial natriuretic peptide (ANP) and anti–TGF-β1 rabbit polyclonal antibodies (Santa Cruz Biotechnology, Santa Cruz, CA); and anti–collagen III, anti–stem cell factor (SCF), and anti–glyceraldehyde-3-phosphate dehydrogenase (GAPDH) goat polyclonal antibodies (Santa Cruz Biotechnology). We used 10% sodium dodecyl sulfate-polyacrylamide gel electrophoresis (SDS-PAGE) used to separate the proteins to analyze AS, cyclin D1, SCF, and GAPDH. We used 15% SDS-PAGE for analysis of ANP and TGF-β1, whereas 7.5% SDS-PAGE was used for analysis of collagen III. After incubation with primary antibody, the bound antibody was visualized with respective horseradish peroxidase (HRP)-coupled secondary antibody (Santa Cruz Biotechnology) and chemiluminescence-developing agents (ECL Plus, Amersham, Piscataway, NJ).

Immunohistochemistry. Formalin-fixed, paraffin-embedded midventricle sections were used for immunohistochemical staining. After overnight incubation with anti–tumor necrosis factor (TNF)-α goat polyclonal antibody (Santa Cruz Biotechnology) at 4°C, the slides were washed in Tris-buffered saline, and then they were reacted with a respective HRP-conjugated secondary antibody (Santa Cruz Biotechnology) at room temperature for 45 minutes. The immunostaining was visualized with the use of diamino benzidine tetrahydrochloride, and the slides were counterstained with hematoxylin. The slides were examined for brown coloration, as an index of immunopositivity, under a high-power light microscope. Quantitation of immunopositivity for TNF-α was done by using higher magnification fields.

Estimation of the Inhibitory Potency of TY-51469 on Simian Chymase or Human Chymase. Simian chymase used was obtained from the heart of rhesus monkey (Charles River Japan Inc.) through purification in accordance with a human heart chymase purification method (18), and human chymase used was obtained from silkworms infected with baculovirus in which a gene that encoded human chymase had been integrated (19). Chymase activity was measured by reacting free His-Leu together with Ang II and OPT to prepare a fluorescent derivative and then by determining the amount quantitatively by means of a fluorophotometer.

First, 3.6 μmol of TY-51469 was weighed in a test tube and was dissolved in 3 ml of dimethyl sulfoxide (DMSO). The DMSO solution was diluted 1000-fold with 20 m*M* Tris-hydrochloric acid buffer solution (pH 8.0) that contained 0.01% Triton X-100 and 0.5 *M* potassium chloride to prepare a 1.2×10^{-6} *M* solution. It was successively diluted with the buffer solution to prepare TY-51469 solutions whose concentrations ranged from 1.2×10^{-6} *M* to 1.2×10^{-9} *M*. To 500 μl of TY-51469 solution of each concentration or buffer solution we added 50 μl of an enzyme solution, and this underwent 10 minutes of preincubation at 37°C. Then, 50 μl of 0.1 m*M* Ang I solution was added to initiate a reaction. Human angiotensin I (Sigma) was employed as Ang I. The enzyme solution to be used for the reaction was adjusted to hydrolyze about 60% of the substrate under the experimental conditions, and the reaction wherein a buffer solution contained no enzyme was carried out as a blind test. After 120 minutes of incubation at 37°C, the reaction was terminated by adding 900 μl of 15% trichloroacetic acid. Thereafter, the reaction mixture was centrifuged at 3,000 rpm for 10 minutes at 4°C, and 2 ml of 2 *M* sodium hydroxide and 1 ml of methanol were added to 1 ml of the resulting supernatant. Then 100 μl of the methanol solution that contained 1.2 mg of *N*-acetyl-L-cysteine and 1 mg/ml OPT was added; thus, a derivatization reaction was initiated. After the reaction mixture was left standing for exactly 1 hour, the fluorescence intensity at the fluorescence wavelength of 502 nm under the excitation wavelength of 304 nm was measured. The measurement was repeated twice for each sample and blind test. The fluorescence intensity obtained by subtracting the average value at the blind test from the average value thereof was determined as chymase activity. An enzymatic reaction in which a buffer solution instead of a TY-51469 solution was used served as a control, and the inhibitory ratio of chymase activity was determined as a percentage by using the chymase activity of the control to divide the difference between the activity at the addition of TY-51469 and the chymase activity of the control. On the basis of each inhibitory ratio, we calculated the IC_{50} value (i.e., the concentration at which 50% of the activity was inhibited).

Stability Study of TY-51469 in Rat Plasma. Seven-week-old male Sprague-Dawley rats were anesthetized with ether in overnight fasting conditions. By abdominal incision, blood was collected from the abdominal aorta by using a heparinized disposable plastic syringe. The blood was centrifuged under cooling to collect supernatant plasma. The collected plasma was frozen and stored at

–30°C and was melted before use. After TY-51469 was dissolved in DMSO, the solution was added to 200 µl of plasma to achieve a concentration of 10 µg/ml and then incubated at 37°C. After 60 minutes, the mixture was acidified by adding 200 µl of 0.1 *M* hydrochloric acid and then extracted twice with 2 ml of ethyl acetate. The resulting organic layer was evaporated to dryness under a nitrogen gas flow, and the residue was dissolved in 200 µl of acetonitrile to prepare a sample solution. In contrast, the test compound was dissolved in a 1% acetonitrile solution of DMSO to achieve a concentration of 10 µg/ml and to serve as a control solution. The sample solution and control solution were investigated by high-performance liquid chromatography. The residual ratio (%) was determined by dividing the peak area of the sample solution with the peak area of the control solution

Toxicity Study of TY-51469 in Rats. The 2-week intravenous repeated-dose toxicity study of TY-51469 was conducted in male Sprague-Dawley rats at daily doses of 0 (control), 20, and 60 mg/kg.

Statistical Analysis. Data are presented as the mean ± the standard error of the mean (SEM). Statistical assessment of the groups was performed by one-way analysis of variance, which was followed by the Tukey or Bonferroni methods of posthoc analysis. The Kruskal-Wallis test was used to analyze the survival times (in the present study data for multiple groups were available). Differences were considered significant at $P < 0.05$.

Results

Inhibitory Potency of TY-51469 on Simian Chymase or Human Chymase. TY-51469 showed good potency in inhibiting simian chymase and human chymase. The IC_{50} values for simian chymase and human chymase were 0.4 n*M* and 7.0 n*M*, respectively.

Stability of TY-51469 in Rat Plasma. The compound TY-51469 showed 100% stability in rat plasma at 40°C for as long as 1 hour.

Results of Toxicity Studies. Results of toxicity studies showed a good profile, even when doses of 20 or 60 mg/kg were administered intravenously. There were no undesired effects on survival rate, clinical signs, BW, and food and water consumption. Ophthalmologic, hematologic, and gross pathological examination showed no abnormalities. Decreases in serum potassium and increases in urine *N*-acetyl-β-D-glucosaminidase excretion were noted in the 60 mg/kg/day group. Increases in absolute submandibular gland weight were recorded for the 20 and 60 mg/kg/day groups without any apparent morphologic changes in the submandibular glands. Histopathological examination revealed the regeneration of renal tubules characterized by cytoplasmic basophilia, increased nucleus-to-cytoplasm ratio, and lymphocytic infiltration in kidneys in the 60 mg/kg/day group. An increase in infiltration of eosinophils in the stomach was observed in one of four rats in the 60 mg/kg/day group. Although these changes may be related to TY-51469 treatment, the degree of these changes was minimal or mild.

Survival Rates. Six (40%) of 15 rats in group V, 4 (27%) of 15 rats in group CYI-0.1, and 3 (20%) of 15 rats in group CYI-1 died between days 30 and 56 of immunization. The survival rate of group CYI-1 was significantly higher than that of group V ($P < 0.05$). The survival rate of group CYI-0.1 was also improved in comparison with that of group V; however, this difference did not attain statistical significance. The normal rats were healthy and alive throughout the protocol.

Myocardial Fibrosis. Fibrosis in the DCM hearts was clearly visible as blue rather than red (normal) regions of the heart (Fig. 1B). Group V showed a significant increase in the percent area of myocardial fibrosis in relation to that of group N (Fig. 1A, B, and Fig. 2A). The percent area of myocardial fibrosis was lower in group CYI-1 than in group CYI-0.1 (Fig. 1C, D, and Fig. 2A). Of the treatment groups, group CYI-1 showed a statistically significant reduction in the percent area of fibrosis when compared with that in group V; however, group CYI-0.1 also showed a trend of decline (Fig. 2A).

Myocardial Hypertrophy. The ratio of HW to BW and the mean cardiomyocyte area, markers of hypertrophy, were greater in group V than in group N. Treatment with a higher dose of the chymase inhibitor (group CYI-1) significantly decreased the ratio of HW to BW; the lower dose (group CYI-0.1) also decreased the ratio of HW to BW, but the decrease was not statistically significant (Fig. 2B). In contrast, the mean cardiomyocyte area was significantly decreased in a dose-dependent manner with chymase inhibitor treatment (Fig. 2C).

Cardiac MCD. Cardiac MCD was significantly greater in the group V samples than in the group N samples (Fig. 1E, F, and Fig. 2D). Treatment with the chymase inhibitor decreased the cardiac MCD in comparison to that in vehicle-treated rats. The reduction in cardiac MCD was higher in the myocardial sections of group CYI-1 than in those of group CYI-0.1 (Fig. 1G, H, and Fig. 2D).

Histamine Concentration in Heart Tissue. The concentration of histamine in wet heart tissue has been designated as an index of cardiac MCD. The concentration of histamine in wet heart tissue of group V was significantly higher than that of group N (Fig. 2E). In the groups CYI-0.1 and CYI-1, the histamine concentration was less than that in group V (Fig. 2E). In these two treatment groups, the group CYI-1 attained a statistically significant difference in comparison with group V (Fig. 2E).

Chymase Activity in Myocardium. Midventricle sections from group V showed greater chymase activity than did those of group N (Fig. 1I, J, and Fig. 2F), whereas chymase inhibitor treatment attenuated it dose-dependently (CYI-0.1 [Fig. 1K, Fig. 2F]; CYI-1 [Fig. 1L, Fig. 2F]).

TNF-α Levels in the Myocardium. Immunostaining showed greater myocardial levels of TNF-α in the

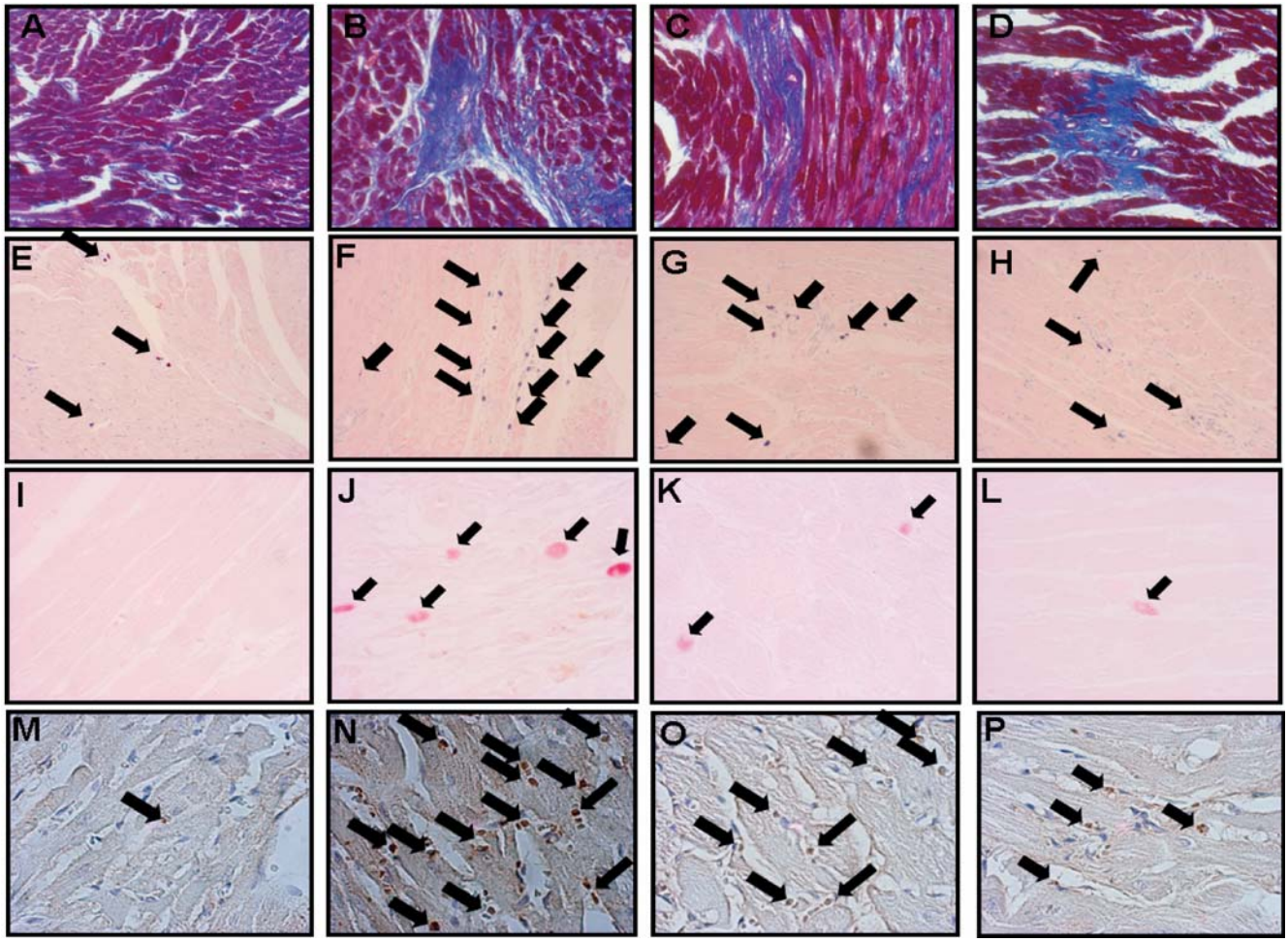

Figure 1. Effect of TY-51469 on myocardial fibrosis. Photographs of the Azan-Mallory–stained midventricle sections of (A) group N, (B) group V, (C) group CYI-0.1, and (D) group CYI-1 under a light microscope are shown. The blue fibrotic area opposed to red myocardium can be viewed in the photomicrograph. Magnification: ×100. Effect of TY-51469 on cardiac MCD in (E) group N, (F) group V, (G) group CYI-0.1, and (H) group CYI-1. More toluidine blue–positive mast cells are in group V than in group N. Treatment groups (i.e., groups CYI-0.1 and CYI-1) show a reduction in cardiac MCD. Toluidine blue–positive (bluish or violet) mast cells are shown by black arrows. Magnification: ×100.Effect of TY-51469 on chymase activity in myocardium in (I) group N, (J) group V, (K) group CYI-0.1, and (L) group CYI-1. Myocardial sections of group V show increased chymase activity in comparison with those of group N, whereas chymase inhibitor treatment decreased it dose-dependently (CYI-0.1 and CYI-1). Black arrows point to areas of pinkish red, signs of positive reactions for chymase activity. Magnification: ×400. Effect of TY-51469 on myocardial TNF-α levels in (M) group N, (N) group V, (O) group CYI-0.1, and (P) CYI-1. Midventricle sections of group V show increased immunohistochemical staining of TNF-α in comparison with those of group N, whereas the chymase inhibitor treatment decreased it dose-dependently (CYI-0.1 and CYI-1). Black arrows point to brown immunopositivity of TNF-α. Magnification: ×400. Representative photomicrographs of each group are shown.

midventricle sections of group V than in those of group N (Fig. 1M, N, and Fig. 2G). A dose-dependent reduction was observed in the treatment groups (CYI-0.1 and CYI-1). However, group CYI-1, but not group CYI-0.1, attained a statistically significant difference (Fig. 1O, P, and Fig. 2G).

Myocardial Functional Parameters. Hemodynamic and echocardiographic analyses revealed the systolic and diastolic function of the myocardium (Fig. 3). The systolic functional parameters (LVP, max. dP/dt, and percent FS) were significantly decreased. The LVDs was significantly greater in group V than in group N, whereas a dose-dependent improvement was observed in the treatment groups (Fig. 3A, C, F, and G). The diastolic parameters LVEDP and LVDd were increased in group V in relation to those in group N, whereas treatment with the chymase inhibitor decreased them dose-dependently (Fig. 3B, E). LVEDP values showed statistical significance between groups, but LVDd readings did not attain statistical significance as shown in Figure 3B and 3E. At the same time, min. dP/dt, another diastolic parameter, was significantly improved in a dose-dependent manner with chymase inhibitor treatment, and was decreased in rats with DCM in comparison with their normal counterparts (Fig. 3D).

Myocardial Levels of AS, SCF, Cyclin D1, TGF-β1, Collagen III, and ANP. The levels of AS, SCF, cyclin D1, TGF-β1, collagen III, and ANP in the myocardium were significantly upregulated in group V as compared with those in group N. After treatment with the chymase

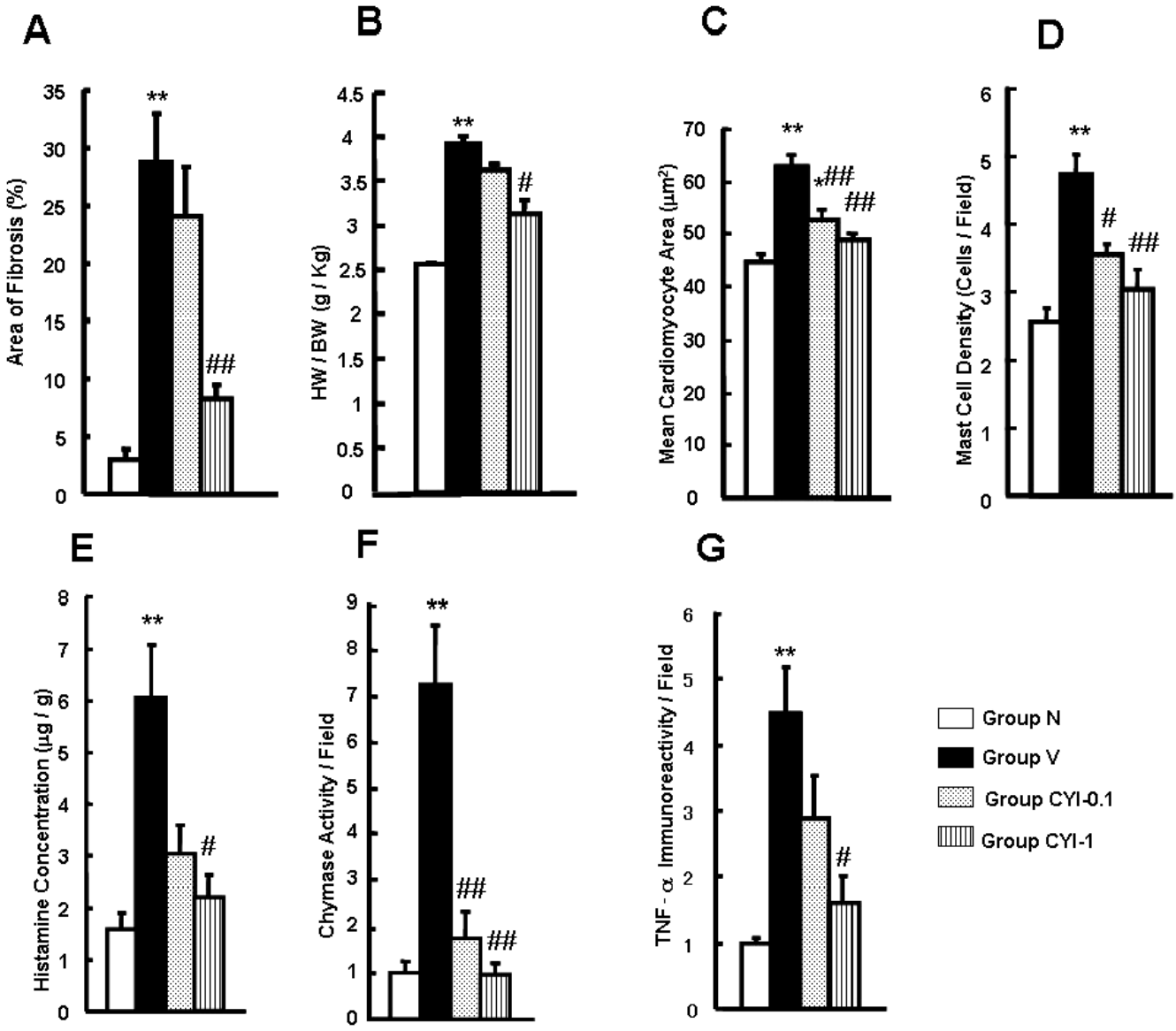

Figure 2. Effect of TY-51469 on (A) the percent area of fibrosis, (B) the ratio of HW to BW, (C) the mean cardiomyocyte area, (D) the cardiac MCD, (E) histamine concentration, (F) chymase activity, and (G) TNF-α level. Values in chymase activity and TNF-α were normalized to those of group N. All values are expressed as the mean ± SEM. Data were obtained from three to five samples. * $P < 0.05$ and ** $P < 0.01$ when compared with data for group N; # $P < 0.05$ and ## $P < 0.01$ when compared with data for group V.

inhibitor, the levels of AS, SCF, cyclin D1, TGF-β1, collagen III, and ANP in the myocardium were significantly attenuated (Fig. 4). However, the statistical significance in the treatment groups differed with different proteins as indicated in Figure 4.

Discussion

To clarify the role of chymase, independent of the Ang II pathway, in the progression of heart failure, we treated postmyocarditis rats with TY-51469, a novel chymase inhibitor, because rat chymase is known for its inability to convert Ang I to Ang II. TY-51469 has good inhibitory potency on chymase. It exhibited 100% stability in rat plasma and a good toxicity profile. The treatment decreased myocardial remodeling, its marker molecules, and mast cell activity; thereby, myocardial function and survival rate improved. As dose selection is an important aspect of the treatment protocols, we considered the drug's solubility and performed a pilot study. Finally, we decided to use doses of 0.1 and 1 mg/kg in our protocol.

Chymase inhibition prevents myocardial fibrosis and improves cardiac function in experimental animals (7, 20). In the chronic phase of autoimmune myocarditis (from day 28 of myosin immunization), the occurrence of fibrosis and hypertrophy is an important cause of myocardial dysfunction. To define the role of chymase in the remodeling process after autoimmune myocarditis, we examined fibrosis and hypertrophy. We also measured levels of cyclin

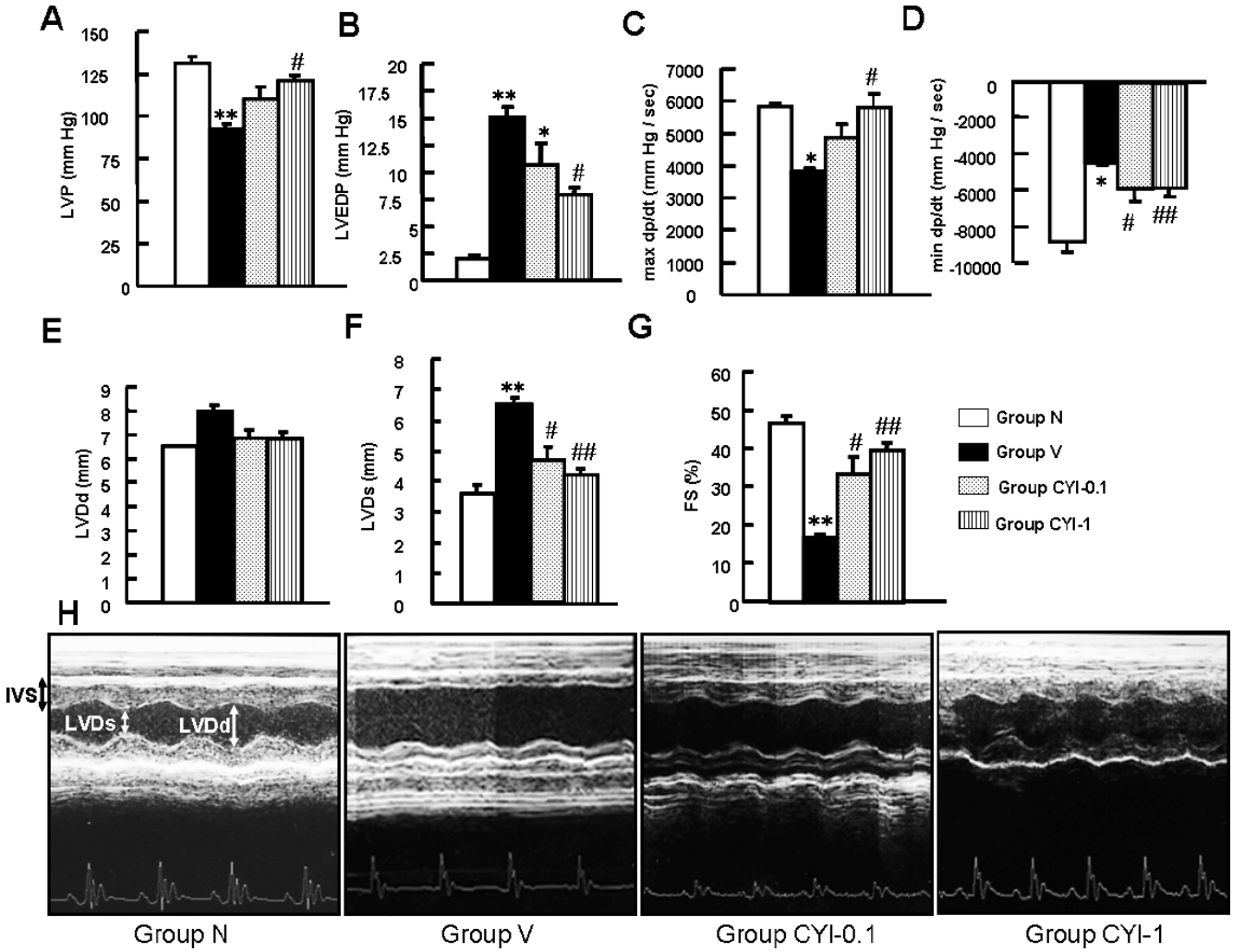

Figure 3. Effects of TY-51469 on the following hemodynamic parameters are shown: (A) LVP, (B) LVEDP, (C) max. dP/dt, and (D) min. dP/dt. Effects of TY-51469 on the following echocardiographic parameters are shown: (E) LVDd, (F) LVDs, and (G) percent FS. All values are expressed as the mean ± SEM. Data from three to five samples are shown. * $P < 0.05$ and ** $P < 0.01$ when compared with data for group N; # $P < 0.05$ and ## $P < 0.01$ when compared with data for group V. (H) Representative M-mode echocardiograms of groups N, V, CYI-0.1, and CYI-1 are shown.

D1, because it has been designated an index of fibrogenesis in heart failure (21). Treatment with the chymase inhibitor decreased the percent area of fibrosis in the myocardial sections that underwent Azan-Mallory staining, the myocardial levels of TGF-β1 and collagen III (the molecular markers of fibrosis), and fibrogenesis as evident from reduced cyclin D1 levels. The ratio of HW to BW, the mean cardiomyocyte area, and ANP, a molecular marker of hypertrophy, were decreased with chymase inhibitor treatment; these decreases indicated a reduction in hypertrophy. Chymase inhibition suppressed myocardial remodeling and ultimately led to improvement in myocardial function as shown by our results. Because rat chymase lacks the ability to generate Ang II (12–14), we found no significant difference in myocardial Ang II levels among the treated and untreated groups (data not shown). Documented evidence suggests that increased expression of AS in the myocardium of rats after myocardial infarction (MI) contributes to post-MI ventricular remodeling (22). It has been suggested that an increase in myocardial AS and aldosterone is involved in myocardial remodeling (23). Hence, finding the involvement of myocardial AS in the present scenario might suggest a new explanation for the mechanism of the chymase-mediated remodeling. Experimentally, increased aldosterone induces pericoronary inflammation and cardiac fibrosis (23). When we analyzed mast cells in myocardial sections, usually we found them adjacent to coronary blood vessels (Fig. 2E–H). Degranulation of mast cells is an integral part of the pathogenesis in this animal model in which chymase is also released. The contribution of chymase in stimulating AS expression and thereby increasing the aldosterone levels in the myocardium to cause the deleterious effect in the postmyocarditis hearts cannot be ruled out. Moreover, our data showing the dose-dependent reduction in the myocardial AS levels with chymase inhibitor treatment also suggest this possibility.

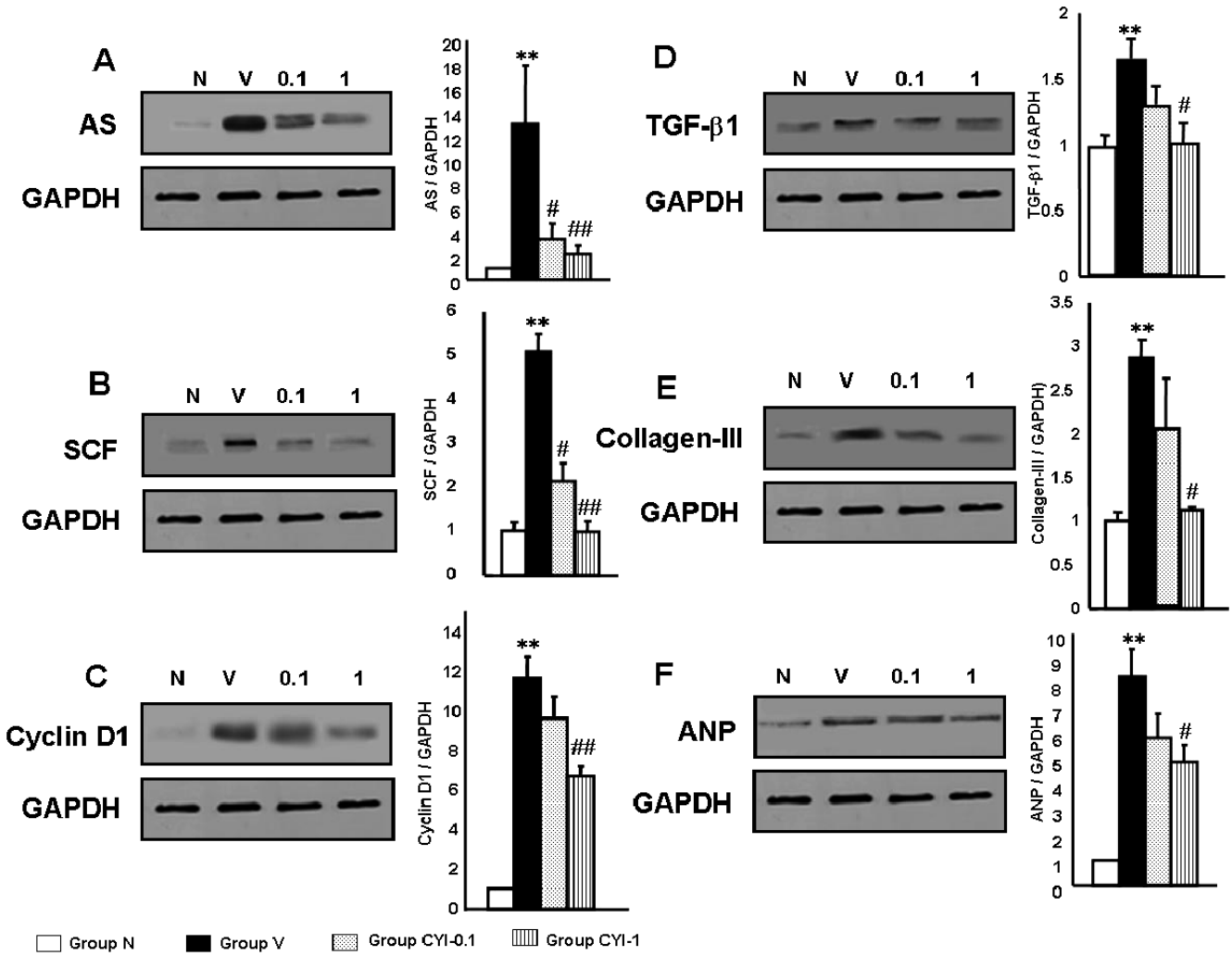

Figure 4. Effect of TY-51469 on myocardial protein levels. Western blot image and quantitation of the following are shown: (A) AS and GAPDH, (B) SCF and GAPDH, (C) cyclin D1 and GAPDH, (D) TGF-β1 and GAPDH, (E) collagen III and GAPDH, and (F) ANP and GAPDH of (lane N) group N, (lane V) group V, (lane 0.1) group CYI-0.1, and (lane 1) group CYI-1. The Western blot image shows representative bands of respective groups. Densitometric analysis of immunoreactive bands for AS, SCF, cyclin D1, TGF-β1, collagen III, ANP, and GAPDH was performed by using Scion Image software, and the results of the quantitation are shown in the graph. Data are the mean signal intensity ± SEM from three to five experiments. The values were normalized to those of group N. ** $P < 0.01$ when compared with data for group N; # $P < 0.05$ and ## $P < 0.01$ when compared with data for group V.

However, these notions should be cautiously interpreted for further steps because the discrepancy about the myocardial AS (24) and elevation in myocardial AS levels may not necessarily lead to the increase in the production of myocardial aldosterone.

Treatment with the chymase inhibitor decreased the degranulating cardiac mast cells, MCD, and histamine concentration. Infiltration, proliferation, maturation (i.e., increased in size and filled with complete granules), and degranulation of mast cells are associated with the progression of myocarditis to heart failure in our model (17, 25). We saw colocalized mast cells in the inflammatory infiltration in postmyocarditis hearts, which suggests that smoldering inflammation exists in postmyocarditis hearts and that the inflammation is an integral part of disease progression (25). Consequently, there is a possibility that the release of inflammatory cytokines from mast cells was suppressed by the chymase inhibitor in the early phase of treatment and decreased the recruitment of inflammatory cells, including mast cells. Our results and hypothesis emulate those of the report of He *et al*., which declared that chymase inhibitors are potent mast cell stabilizers (26). On the basis of our results, we consider that the effects of the chymase inhibitor in the prevention of heart failure were achieved partly through the suppression of mast cell activity.

Cardiac-specific overexpression of TNF-α in mice caused left ventricular hypertrophy and dilation with a concomitant increase in matrix metalloproteinase activity (27). SCF has been suggested to play an important role in the fibrotic cascade in cardiomyopathy (5). Thus, our results showed that the reduction in myocardial levels of TNF-α

and SCF with chymase inhibition may have importance in suppressing the molecular signaling pathways of remodeling events.

In summary, the inhibition of the chymase pathophysiological pathway, independent of Ang II involvement, contributes to the suppression of myocardial fibrosis, hypertrophy, and residual inflammation, thereby leading to the improvement of myocardial function and prevention of heart failure in rats with DCM after autoimmune myocarditis. Finally, it can be concluded that inhibition of chymase reduces the pathogenesis of DCM in rats.

1. McEuen AR, Sharama B, Walls AF. Regulation of the activity of human chymase during storage and release from mast cells: the contributions of inorganic cations, pH, heparin and histamine. Biochim Biophys Acta 1267:115–121, 1995.
2. Galli SJ, Wershil BK. Mouse mast cell cytokine production: role in cutaneous inflammatory and immunological responses. Exp Dermatol 4:240–249, 1995.
3. Church MK, Levi-Schaffer F. The human mast cell. J Allergy Clin Immunol 99:155–160, 1997.
4. Welle M. Development, significance, and heterogeneity of mast cells with particular regard to the mast cell-specific proteases chymase and tryptase. J Leukoc Biol 61:233–245, 1997.
5. Patella V, Marino I, Arbustini E, Lamparter-Schummert B, Verga L, Adt M, Marone G. Stem cell factor in mast cells and increased mast cell density in idiopathic and ischemic cardiomyopathy. Circulation 97: 971–978, 1998.
6. Engels W, Reiters PH, Daemen MJ, Smits JF, van der Vusse GJ. Transmural changes in mast cell density in rat heart after infarct induction in vivo. J Pathol 177:423–429, 1995.
7. Matsumoto T, Wada A, Tsutamoto T, Ohnishi M, Isono T, Kinoshita M. Chymase inhibitor prevents cardiac fibrosis and improves diastolic dysfunction in the progression of heart failure. Circulation 107:2555–2558, 2003.
8. Kunori Y, Muroga Y, Iidaka M, Mitsuhashi H, Kamimura T, Fukamizu A. Species differences in angiotensin II generation and degradation by mast cell chymases. J Recept Signal Transduct Res 25:35–44, 2005.
9. Taniyama Y, Morishita R, Nakagami H, Moriguchi A, Sakonjo H, Shokei-Kim, Matsumoto K, Nakamura T, Higaki J, Ogihara T. Potential contribution of a novel antifibrotic factor, hepatocyte growth factor, to prevention of myocardial fibrosis by angiotensin II blockade in cardiomyopathic hamsters. Circulation 102:246–252, 2000.
10. Hara M, Matsumori A, Ono K, Kido H, Hwang MW, Miyamoto T, Iwasaki A, Okada M, Nakatani K, Sasayama S. Mast cells cause apoptosis of cardiomyocytes and proliferation of other intramyocardial cells in vitro. Circulation 100:1443–1449, 1999.
11. Kitaura-Inenaga K, Hara M, Higuchi K, Yamamoto K, Yamaki A, Ono K, Nakano A, Nakatani K, Sasayama S, Matsumori A. Gene expression of cardiac mast cell chymase and tryptase in a murine model of heart failure caused by viral myocarditis. Circ J 67:881–884, 2003.
12. Yamamoto D, Shiota N, Takai S, Ishida T, Okunishi H, Miyazaki M. Three-dimensional molecular modeling explains why catalytic function for angiotensin-I is different between human and rat chymase. Biochem Biophys Res Commun 242:158–163, 1998.
13. Takai S, Sakaguchi M, Jin D, Yamada M, Kirimura K, Miyazaki M. Different angiotensin II-forming pathways in human and rat vascular tissues. Clin Chim Acta 305:191–195, 2001.
14. Hollenberg NK. Implications of species difference for clinical investigation: studies on the renin-angiotensin system. Hypertension 35:150–154, 2000.
15. Kodama M, Matsumoto Y, Fujiwara M, Masani F, Izumi T, Shibata A. A novel experimental model of giant cell myocarditis induced in rats by immunization with cardiac myosin fraction. Clin Immunol Immunopathol 57:250–262, 1990.
16. Watanabe K, Ohta Y, Nakazawa M, Higuchi H, Hasegawa G, Naito M, Fuse K, Ito M, Hirono S, Tanabe N, Hanawa H, Kato K, Kodama M, Aizawa Y. Low dose carvedilol inhibits progression of heart failure in rats with dilated cardiomyopathy. Br J Pharmacol 2000:1489–1495, 2000.
17. Palaniyandi SS, Watanabe K, Ma M, Tachikawa H, Kodama M, Aizawa Y. Inhibition of mast cells by interleukin-10 gene transfer contributes to protection against acute myocarditis in rats. Eur J Immunol 12:3508–3515, 2004.
18. Urata H, Kinoshita A, Misono KS, Bumpus FM, Husain A. Identification of a highly specific chymase as the major angiotensin II-forming enzyme in the human heart. J Biol Chem 265:22348–22357, 1990.
19. Takai S, Shiota N, Kobayashi S, Matsumura E, Miyazaki M. Induction of chymase that forms angiotensin II in the monkey atherosclerotic aorta. FEBS Lett 412:86–90, 1997.
20. Takai S, Jin D, Sakaguchi M, Katayama S, Muramatsu M, Sakaguchi M, Matsumura E, Kim S, Miyazaki M. A novel chymase inhibitor, 4-[1-([bis-(4-methyl-phenyl)-methyl]-carbamoyl)3-(2-ethoxy-benzyl)-4-oxo-azetidine-2-yloxy]-benzoic acid (BCEAB), suppressed cardiac fibrosis in cardiomyopathic hamsters. J Pharmacol Exp Ther 305:17–23, 2003.
21. Sharma UC, Pokharel S, van Brakel TJ, van Berlo JH, Cleutjens JP, Schroen B, Andre S, Crijns HJ, Gabius HJ, Maessen J, Pinto YM. Galectin-3 marks activated macrophages in failure-prone hypertrophied hearts and contributes to cardiac dysfunction. Circulation 110:3121–3128, 2004.
22. Silvestre JS, Heymes C, Oubenaissa A, Robert V, Aupetit-Faisant B, Carayon A, Swynghedauw B, Delcayre C. Activation of cardiac aldosterone production in rat myocardial infarction: effect of angiotensin II receptor blockade and role in cardiac fibrosis. Circulation 99: 2694–2701, 1999.
23. Heymes C, Garnier A, Fuchs S, Bendall JK, Nehme J, Ambroisine ML, Robidel E, Swynghedauw B, Milliez P, Delcayre C. Aldosterone-synthase overexpression in heart: a tool to explore aldosterone's effects. Mol Cell Endocrinol 217:213–219, 2004.
24. Funder JW. Cardiac synthesis of aldosterone: going, going, gone . . . ? Endocrinology 145:4793–4795, 2004.
25. Palaniyandi Selvaraj S, Watanabe K, Ma M, Tachikawa H, Kodama M, Aizawa Y. Involvement of mast cells in the development of fibrosis in rats with postmyocarditis dilated cardiomyopathy. Biol Pharm Bull 28: 2128–2132, 2005.
26. He S, Gaca MD, McEuen AR, Walls AF. Inhibitors of chymase as mast cell-stabilizing agents: contribution of chymase in the activation of human mast cells. J Pharmacol Exp Ther 291:517–523, 1999.
27. Li YY, Feng YQ, Kadokami T, McTiernan CF, Draviam R, Watkins SC, Feldman AM. Myocardial extracellular matrix remodeling in transgenic mice overexpressing tumor necrosis factor alpha can be modulated by anti-tumor necrosis factor alpha therapy. Proc Natl Acad Sci U S A 97:12746–12751, 2000.